

Simulation Calibration of an Extensive Air Shower array, by a logged data set of its small prototype

M. Khakian Ghomi

Energy engineering and physics department, Amirkabir univ. of tech., 15875-4413, Tehran, Iran; email: khakian@aut.ac.ir

Abstract. Alborz observatory is an EAS array in the heights of Alborz mountain chain near Tehran. For the development of the array, more number of detectors is inevitable. The managing the financial resources and achieving the highest efficiency of the array is important for the project. Therefore, Water Cherenkov Detectors has been used for 9 months in the same way as the previous experiment with Scintillation Detectors in a 4-fold square arrangement. After a hardware calibration procedure, the experimental data set was simulated by CORSIKA code and the experimental restrictions were applied over the data set. In this work, the simulation is calibrated with the real experimental results, and it presents a comparable parameter between the experiment and the simulation. The obtained results show that the simulation is in agreement with the experimental results.

Keywords: Extensive Air Shower (EAS), Cosmic Rays, Water Cherenkov Detector(WCD)

1 Introduction

Alborz observatory² is an Extensive Air Shower (EAS) array of particle detectors, in the range of UHE cosmic and gamma rays, located near Tehran ($35^{\circ}N$, $51^{\circ}E$) at an altitude of 2650m a.s.l. Based on the models of EASs, the altitude is around the shower maximum of Cosmic Ray(CRs) with 10^{17} to 10^{18} eV [1, 2, 3, 4, 5]. In this energy range and with the area of the observatory ($\sim 2 \times 10^5$ m²), detection rate is a very rare event [3]; but the array is able to detect lower energy CRs[3]. Lower threshold energy of a prototype array of a 4-fold square shaped NaI scintillation detectors, is about 5×10^{13} to 10^{14} eV[6, 7]. The development of the array in a larger area with more number of detectors increases the event rate and makes more accurate results due to its more rich data[8]. Many aspects of particle scintillation detector(SD) parameters and their effects on the detection efficiency have been the subject of many studies[9, 10]. To apply more detectors in the array, it is needed to have a suitable simulation for the experiment. Since large number of SDs cost too much, they are not an accessible choice for the future plan of the observatory. Water Cherenkov Detector (WCD) is a less expensive alternative. The alternative is sometimes used by other scientists for detection of charged particles via detection of cherenkov radiation inside water[11, 12, 13]. The WCD is a cylindrical water tank, which is more accessible and cheaper in comparison with the SDs. Therefore, the detector was studied with more details in some independent experiments for the WCD individually[14, 15]. In the next step, its operation investigated in an array of WCDs similar to the SD array[6] because there was a good experience with the array of SDs[15, 16, 19, 20].

²<http://www.sina.sharif.ir/observatory>

In fact, this work, tries to answer the question: " *Could the WCDs be as confident as SDs in the array arrangement?* ".

Obtained results from the WCD experiment, showed a good agreement with the SD experiment. Of course there are some differences which are mostly due to the different geometry and different detection procedures of WCDs and SDs[6].

Detection mechanisms of charged particles by SDs and WCDs are quite different[21]. The arrangement of the two arrays (SDs and WCDs) are the same but dimensions of the WCDs are different from SDs. Target of this work, is the calibration of the simulation, by the obtained results of the prototype WCD experiment.

In the 2nd section, the experimental arrangement is briefly introduced. 3rd section studies the error estimation of the experiment. In section 4, simulation procedure of the experimental events is presented in two steps; generation of the events by CORSIKA code[24] and application of the experimental restrictions over the simulated events. The fifth section compares the results of the simulation and the experiment. And finally in the last section, some discussions about the results and future plans are presented. Also in this section, few comments been proposed to have more efficient simulations in the future.

2 Experimental arrangement

A 4-fold square array of WCDs with the side of 6.08m is located on horizontal surface of the physics department roof at Sharif University of Technology (35°43'N, 51°20'E, 1200m \equiv 890 gr/cm²). Each detector is a cylindrical metallic reservoir painted white inside, with 64cm diameter and 120cm height, it contains about 380 liters of sealed water (Figure 1a). There is a 52mm EMI 9813B PMT (www.electrontubes.com) faced inside water[6] at the center of upper surface of the WCDs.

If at least one charged particle passes through the water, its Cherenkov blue light radiation (in the range of 470nm) is enough to turn the PMT on[14]. An investigation on a single WCD has shown that more than 90% of particles passing through the WCD are detectable[15]. The PMT output pulse height is related to:

i) direction, *ii*) number and *iii*) location of the passed particles through each WCD[15].

The used PMTs have amplification factor of 1×10^8 and its supporter electronics is a set of NIM modules and a Multi Channel Analyzer(MCA) (Figure 1b). It is used 4 fast Discriminator (CAEN N413A) operating at fixed levels around 35mV to 200mV. The thresholds are set to separate signals from background noise. The 4 Discriminator outputs fed into 3 Time to Amplitude Converters (TAC)(EG&G ORTEC 566) which are set to 200ns full scale (Maximum acceptable time differences between each two WCDs). Therefore, it is obtained 3 Δt s (Δt_{31} , Δt_{32} and Δt_{34}) which are fed into 3 TACs (1 to 3 in Figure 1b). Meanwhile it was recorded true time (GMT) of each EAS event (T_{GMT}) with the accuracy of synchronized computer with the site www.timeanddate.com. TAC outputs are fed into a Multi parameter MCA (KIAN AFROUZ Inc.) via an Analogue to Digital Converter (ADC)(KIAN AFROUZ Inc.). The first triggered case is on the first parameter (Δt_{31}). When it turns on, the event will be recorded and selection of true events is postponed to off-line parts. Usually in large arrays there are some problems like memory and off-line processing ones with the recorded large data sets. Since our experimental arrangement has not the problems, therefore, it was applied a soft trigger case to record the events. Meanwhile, this condition needs a poor logic and less electronic modules too. A total of 30 experiments have recorded 1,768,195 events in 12,258,670.0 seconds for about nine months. Off-line triggering condition has eliminated any event which has any null Δt 's. This step eliminated most of the useless events. Some more refinements are used to improve the accuracy of the data set. Finally it was obtained

476,675 true EAS events ($\sim 27\%$) with the rate of 0.0389 Hz. In section 4.2.2 the number of triggered cases is applied on the simulation. The number of triggered cases in the simulation is: *turn on all of the 4 detectors on a square configuration like the experiment.*

3 Error investigation

3.1 Independency of the experimental events

Primary cosmic rays with different sources miss their directions due to the magnetic field or other effects on their path. When an EAS is recorded, it is expected that the event should be quite independent from the other recorded events. To verify the in-dependency, the rate and time separation between consequent events were studied. These sequential events are between each two, three, four, five and six member sequences.

Figure 2(a) shows the distribution of time differences between each two consecutive events (Δt_1) which has a good agreement with exponential distribution function $F(\lambda_1) = A \exp(-\lambda_1 \Delta t_1)$ with $\lambda_1 = 0.0391$ Hz. Meanwhile, it is obtained $\Delta t_m = t_i - t_{i-m}$ with ($m=$) 2, 3, 4 and 5. Figure 2(b) shows a good agreement between the obtained results and Gamma-Function

$$G(\Delta t_m, \lambda_m, m) = \frac{\Delta t_m^{m-1}}{(m-1)!} N \lambda_m^m \exp(-\lambda_m \Delta t_m) \quad (1)$$

where $\bar{\lambda} = 0.0395 \pm 0.0002$ Hz for the obtained 5 λ s. Therefore, the events are quite random. CORSIKA code uses a random generator with 10^9 sequence length loop for generation of simulated events[24] which guarantees the in-dependency of the events.

3.2 Angular resolution of the experiment

Calculated errors of the array with scintillation detectors are investigated from error propagation of all of experimental parameters over the angular resolution of the experiment which is 5.0° [16]. In the WCD, error propagation procedure, causes $7.2^\circ \pm 1.0^\circ$ for the angular resolution of WCD array[6]. The different angular resolutions of the the SD and WCD arrays, are due to the different geometries and dimensions of the SDs and WCDs. In follow, it seems that it is better to use a binning with at least 6.2° intervals. Since in the SD experiment[16] it has been calculated error of the experiment by error propagation procedure equal to 5.0° and after it, in another work, but with the data set and with moon shadow effect, it has been obtained 4.5° [17] angular error. Therefore, in this investigation it is used a smaller 5° binning for the events.

4 Simulation of the experimental events

The simulation contains two parts:

The first one is generation of some CORSIKA simulated events(SEs) comparable with the number of experimental events. It should be suggested that the creation time of the data set with a normal PC was as long as the experimental duration itself.

In the second part of the simulation, the experimental constrains were applied to the created events. In this part the calculations over the simulated data set are exactly the same as calculations on the data set of the real experimental events.

4.1 Generation of the CORSIKA simulated events

A sum of 392,200 CORSIKA (V6204 code) events were simulated for a flat surface[24]. GHEISHA and QGSJET models were used for low and high energy ranges of hadronic interactions respectively. Below the knee, about 90% of primary cosmic rays are Protons, 10% are α particles (Helium nucleus) and less than 1% contains heavier elements[3, 21, 25]. Therefore, it was considered the primary cosmic ray composition (90%,10%,0%) in the simulation.

These SEs are created for the array site (University site) with 1200 m a.s.l., $B_x = 28.1 \mu\text{T}$ and $B_z = 38.4 \mu\text{T}$ (Figure 1), and energy distribution power is $dN/dE \propto E^{-2.7}$.

Azimuth angles of the SEs are from 0 to 360° uniformly. CORSIKA random generator considers $dN/d\theta = A \sin \theta \cos \theta$ for zenith angle distribution of the SEs[24]. Zenith angle of the SEs were considered from 0 to 60° .

Lower and higher energy thresholds of the simulation were considered as 50 TeV[16] to 5 PeV (few events per experimental duration) without thinning. Also as an input information for the simulation, it was considered energy cuts for hadrons, muons, electrons and photons 0.3, 0.3, 0.003 and 0.003 GeV, respectively.

4.2 Application of the experimental restrictions over the SEs

This part was divided into three sub-parts.

- i)* Calculation of effective surface of the WCD for each SE, individually.
- ii)* Application of experimental trigger condition over each SE.
- iii)* Finding a comparative parameter to compare the simulation and experimental results.

4.2.1 Calculation of effective surface of the WCDs for each SE

CORSIKA code creates SEs for a flat surface and flat detectors[24]. The generated EAS events, are recorded in a square format with the accuracy of 1cm. Therefore, it is needed to calculate the equivalent effective surface of the WCDs as a flat square detector in different angles. Since the WCDs are 3 dimensional, effective surface of the WCDs depends on zenith angle of the events (Figure1c), therefore, zenith distribution function of the events will be:

$$dN/d\theta = A \sin \theta A_{eff}(\theta) \cos^{(n-1)} \theta. \quad (2)$$

Where "A" is the proportionality constant, $\sin \theta$ is due to the FOV of the array; A_{eff} is the effective surface of the WCD, and $\cos^{n-1} \theta$ is due to the atmospheric thickness effect[6]. The effective surface $A_{eff}(\theta)$ is:

$$A_{eff} = P_0 A_0 \cos \theta + P_{90} A_{90} \sin \theta \quad (3)$$

where A_0 and A_{90} are surfaces of the WCD for 0° and 90° zenith angle events respectively. Also P_0 and P_{90} are detection probabilities in these angles where $P_0/P_{90} = 2.1$ [15].

4.2.2 Application of trigger case over each SE

An EAS event (in 50 TeV to 5 PeV energy ranges) extends on a vast region on the ground (more than a few kilometers in radius) but there is a very low surface density at larger radii. A large square array composed of cells of size A_{eff} are considered as a Simulated Detector Array (SDA)(Figure 3). The center of each SE is projected on the center of the related SDA. In an independent simulation for one of the WCDs[15] it is obtained that the response of the WCD for a charged particle is more than 90%[23]. Therefore, in the SDA the response

of each virtual WCD (VWCD) is considered to be 1. It is assumed that if a charged particle passes through a VWCD, it will be detected.

Trigger condition for each SE is the same as in section 2. In the experiment, an event is accepted if all of the 4 WCDs record, passing of at least one charged particle. Now in the simulation, the condition is applied again for VWCDs. If an EAS event satisfies at least one square configuration like the experiment (Figure 3 shows 2 triggered cases) essentially it might be detected by the array, and if the number of the triggered cases increases, detection probability will be increased. From the projected data over VWCDs, it is possible to calculate zenith(θ) and azimuth(ϕ) angles of each SE, exactly the same as calculations for the experimental events[6]. In this method, it has been calculated zenith and azimuth angles (θ, ϕ) of each SE by least square method[26, 27].

Since the number of VWCDs increases with the second power of the SDA size, it is efficient to obtain a better estimation about the size of the SDA before starting the simulation. Since it should be estimated the SDA size for all of the SEs, therefore, it was calculated a weighted mean size $\bar{l}_{WCD} = \sqrt{\bar{A}_{eff}}$, which is used for mean length of each VWCD with the mean area of \bar{A}_{eff} in the SDA:

$$\bar{A}_{eff} = \frac{\int_0^{\pi/3} (P_0 A_0 \cos \theta + P_{90} A_{90} \sin \theta) \sin \theta d\theta}{\int_0^{\pi/3} \sin \theta d\theta} = 0.65 \text{ m}^2. \quad (4)$$

\bar{l}_{WCD} is equal to $\sqrt{0.65} = 0.81\text{m}$.

Therefore, it was calculated mean density of particles per each VWCD for 50,000 random SEs, vs. radius from shower core. Figure 4 shows density of charged particles per each VWCD. At $r = 500 \times \bar{l}_{WCD}$ the density about 0.47 particle per A_{eff} . Therefore, probability of trigger cases of the experiment (turning on four VWCDs in a square configuration) becomes less than a few percent in larger radii. Therefore, the SDA was considered 1000×1000 square shaped detectors (Figure 3).

4.2.3 A comparative parameter between the SEs and the experimental events

Thickness of EAS front at the center, is less than a meter (\sim a few ns) and at the outer regions around a few meters (\sim a few 10ns)[1, 3, 21, 28]. In the 4-fold WCD experiment Δt s at the order of ten nanoseconds, in a TAC duration of 200ns (more details in section 2). TAC starts when the first particle of EAS front passes through the start detector and it stops when the stop detector receives its first particle. Therefore, the experiment is only able to detect the first particle passes through each WCD. So in the SDA, it will be recorded only time of the first particles hits on each VWCD.

Now the experimental trigger condition is applied for the SDA from the first VWCD (up-right corner pixel (-500,-500)) until the last one (bottom-left corner (500,500)) (Figure 3) and scans all the SDA. Number of triggered squares (N_{trig}) over each SE, could be a parameter to compare the SE and a real EAS event. The parameter seems to be related to detection probability of the SE. In each SE "the number of triggered cases", was calculated a direction. For each SE there are N_{trig} independent directions (θ s and ϕ s). Since detection efficiency of the charged particles is high, therefore, the edge of the front will be detected and the calculated directions of the shower by a small array is on the normal to the shower edge. Therefore, when it is averaged over all of the directions of the triggered conditions, the directions are axisymmetric and the distribution of the obtained directions around the primary direction is a symmetric peak function[30, 31] and may be there is a large error bar for the obtained direction, but the real direction of the EAS is near to the average. Since it is not well known which of the squares is matched on the experimental arrangement, therefore,

average of the directions is considered as the direction of the SE and standard deviation of the directions will be angular resolution of the SE. To calculate the angular resolution of the events in each 5° bins, it is calculated $\bar{\sigma} = \sqrt{\sum \sigma_i^2 / N}$, where σ_i is angular resolution of each SE and N is the number of SEs in each 5° bin. This is due to the stochastic nature of the CORSIKA SEs specially by hadronic primary particles and their conic front shape.

5 Experimental and Simulation results

The first subsection is specified the N_{trig} as detection probability, then in the next subsections the parameter is used for comparisons between the simulation and the experiment. Importance of the parameter N_{trig} , depends on the compatibility of the simulation predictions and experimental results.

5.1 Specification of N_{trig} with comparison of the experiment and simulation

On each SE, all of the triggered cases over the SDA are considered one by one. From the N_{trig} conditions in each SE, N_{trig} number of θ s and ϕ s are obtained. Therefore, $\bar{\theta} \pm \sigma_\theta$ for zenith angle of each SE were calculated as follows:

$$\bar{\theta} = \frac{1}{N_{trig}} \sum_{i=1}^{N_{trig}} \theta_i, \quad \sigma_\theta = \sqrt{\frac{\sum_{i=1}^{N_{trig}} (\theta_i - \bar{\theta})^2}{N_{trig}}} \quad (5)$$

In 11 steps it was applied lower threshold of N_{trig} from 1 to 11 one by one. By fitting the equation 2 on the 11 distribution it was obtained 11 cosine power 'n' which were drawn in Figure 5. By fitting an arbitrary function ($y^2 = a + b \ln x$) with the best fit ($r^2 = 0.99904$) and with $n = 6.8 \pm 0.1$ [6], $N_{trig} = 6.82 \pm 2.11$ was obtained. Therefore, $N_{trig} = 6.82 \approx 7$ shows the most compatible distribution of detectable SEs with the experiment; therefore, $N_{trig} \geq 7$ are considered as detectable SEs.

5.2 Estimation of energy threshold of the experiment by the detectable SEs

To check the number of triggered cases as a candidate for the detection probability in the simulation, it is better to estimate the threshold energy of the SEs with $4.71 \leq N_{trig} \leq 8.93 \equiv N_{trig} \in \{5, 6, 7, 8\}$ ($N_{trig} = 6.82 \pm 2.11$).

In the WCD experiment, threshold energy was $E_{th} \approx 95 \text{ TeV}$ [6]. For estimation of the E_{th} from the simulation, it was averaged over the energy of events with $N_{trig} \in \{5, 6, 7, 8\}$, which in the 392,200 SEs, there are 11,553 events. Average energy and standard deviation of the events are $\bar{E}_{th} \pm \sigma_{th} = 108.09 \pm 117.63 \text{ TeV}$. More detailed is shown in Table 1. It is seen that \bar{E} has small fluctuation between 106.86 and 111.12 for $N_{trig} \in \{5, 6, 7, 8\}$. The large standard deviations are due to:

- i*) the stochastic nature of the simulated events;
 - ii*) large zenith angle events ($40 \leq \theta \leq 60$) with higher energies up to 5 PeV with small N_{trig} .
- Effects of zenith angle and energy will be discussed in subsection 5.3.

N_{trig}	#	\bar{E}	σ_E
5	3538	106.93	126.67
6	3012	111.12	122.41
7	2575	107.32	114.20
8	2428	106.86	100.14

Table 1: Number, Mean Energy and Standard deviation of energy of events(σ_E) with $N_{trig}=5$ to 8 individually. This results show that the threshold energy of the experiment is about 100 TeV.

	N_{tot}	$N_{(0<\theta<40^\circ)}$	$N_{(40^\circ\leq\theta\leq60^\circ)}$	$N_{(40^\circ\leq\theta\leq60^\circ)}/N_{tot}$
SE_{all}	392200	215852	176348	44.96%
$SE_{N_{sq}\geq7}$	109440	100668	8752	8.00%

Table 2: In all of SEs 45% of the events are in the zenith angles $40 \leq \theta \leq 60$ in case that in the detectable events there is only 8% of the total events in zenith angles $40 \leq \theta \leq 60$.

5.3 Zenith angle effect on the parameter N_{trig}

From the 392,200 SEs 242,308 of them are null events and have no triggered cases ($N_{trig} = 0$)! This means that about 61% of the SEs are not detectable at all. So the question is "why is the high fraction not detected?". Average zenith angle of the null events is $\bar{\theta}_0 \pm \sigma_{\theta_0} = 43.55^\circ \pm 11.58^\circ$, in case that, all SEs have $\bar{\theta}_{tot} \pm \sigma_{\theta_{tot}} = 36.56^\circ \pm 14.43^\circ$. Also for 53,212 higher energy null events ($E \geq 100$ TeV), there is $\bar{\theta}_0 \pm \sigma_{\theta_0} = 47.74^\circ \pm 8.67^\circ$ but for 55,217 higher energy ($E \geq 100$ TeV) detectable events with $N_{trig} \geq 7$ there is $\bar{\theta}_{det} \pm \sigma_{det} = 25.91^\circ \pm 11.18^\circ$. Figure 6 shows that higher energy events with larger zenith angles seems to be more fret, and triggered cases become harder for them.

CORSIKA selects the primary zenith angle of the events with the distribution of $\sin \theta \cos \theta$ [24]. Maximum of the distribution $\sin \theta \cos \theta$ is on the 45° and contribution of the total events in the interval $40^\circ \leq \theta \leq 60^\circ$ is about 45%, in Table 2 it is seen that detectable events in the interval are only about 8%. Therefore, as a result:

- i) higher energy events with higher zenith angles make a large uncertainty over the energy threshold.
- ii) for more efficient simulations, it is better to simulate smaller zenith angle events ($0 \leq \theta \leq 40^\circ$).

5.4 Observation of atmospheric optical thickness for detectable events

Secondary particles of real EAS events with higher zenith angles, have longer paths in the atmosphere. So higher zenith angle EAS events have less secondary particles and fret particle densities at the ground[29, 32]. In visible astronomy there is a well known parameter as *air mass* which decreases the light intensity of astronomical sources exponentially with $\sec \theta$ [33]:

$$I = I_0 e^{-\tau_0 \sec \theta}. \quad (6)$$

In the astroparticle field, slant depth ($X = \int \rho dv$) plays the role of air mass in visible astronomy. In the SEs it is expected that increase of zenith angle of the events decreases N_{trig} . Figure 7 shows mean number of triggered case (N_{trig}) for the events with $N_{trig} \geq 7$ for 5° intervals. It is seen that there is a compatibility ($r^2 = 0.93202$) of the equation 6 with $N_{trig}(\theta)$.

	N_{tot}	$N_{(50 \leq E < 100) \text{ TeV}}$	$N_{(100 \leq E < 5000) \text{ TeV}}$	$N_{(100 \leq E < 5000) \text{ TeV}} / N_{tot}$
SE_{all}	392200	271664	120536	30.73%
$SE_{N_{trig} \geq 7}$	109440	54223	55217	50.45%

Table 3: In all of SEs 70% of the events are in the energy range $50 \leq E \leq 100$ TeV it is in case that in the detectable events there is only 50% of the total events are in in the energy range $50 \leq E \leq 100$ TeV.

5.5 Effect of primary energy of SEs on N_{trig}

Figure 8 shows the distribution of the null SEs ($N_{trig} = 0$) near to the lower threshold of the simulation. It is observable that the distribution is decreasing steeply by a power law. Average and standard deviation of these events are $\bar{E}_0 \pm \sigma_0 = 90.78 \pm 78.50$ TeV. It is expected that higher energy events have more secondary particles, so they are more detectable. Figure 9 shows, N_{trig} increases with increase of energy. Higher energy particles have larger number of secondary particles, so detection probability increases with increase of energy. Of course large error bars are due to: *i*) zenith angle effect and *ii*) smaller statistics at higher energies.

Table 3 shows that if 50 TeV threshold energy is replaced by 100 TeV, the simulation will be considered more efficiently.

6 Conclusion

Simulation in experimental researches is the second wing of the experiment. The simulation should be completely harmonized and calibrated by the experiment. In this work to verify the simulation and its calibration, it was used the CORSIKA code to generate of a set of simulated events and compared the obtained results with the experimental ones. It was found a parameter which is "the number of triggered cases" in the simulation (N_{trig}). The obtained results show that the N_{trig} is proportional to detection probability of the experiment. Some results are:

Ri) Higher zenith angle events are less detectable exponentially with $\sec \theta$ similar to *air - mass* effect.

Rii) Energy threshold of the experimental events and the SEs are near to each other.

Riii) The most important obtained result is the compatibility of the simulation with the experiment.

Of course for more accurate analysis in the future, it is better to repeat the simulation more efficiently. Since the generation of the simulated events is a time and memory consuming work, some comments are proposed for the future investigations:

C1) It is more efficient in time and memory to simulate lower zenith angle events ($0 \leq \theta \leq 40^\circ$).

C2) It is better to apply threshold energy equal to 100 TeV, lower than this amount is eliminated

Generated hadronic events by CORSIKA code, have a stochastic nature and their fluctuation is high, therefore, it is better to simulate as much as possible in the future plans for more confidence (specially in the recommended angle and energy domains).

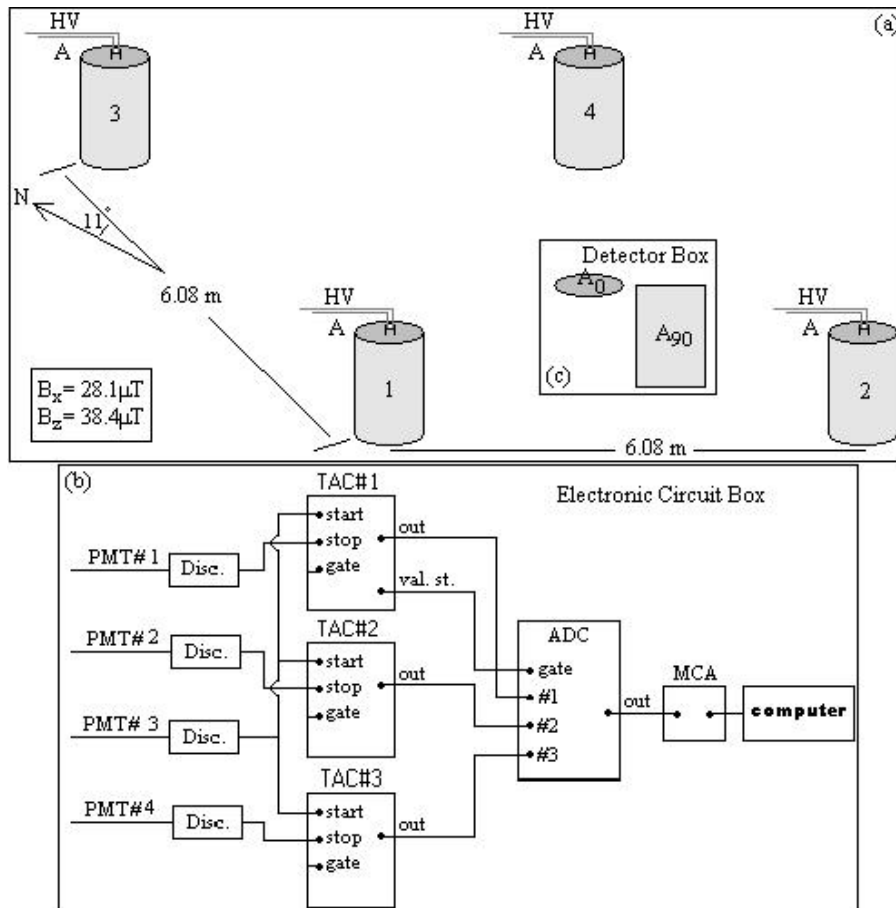


Figure 1: Different parts of the figure respectively show (a): Schematic configuration of the detector array, (b): Data acquisition system and used electronic circuits, (c)(inside a): Vertical (A_0) and horizontal (A_{90}) sections of the WCDs.

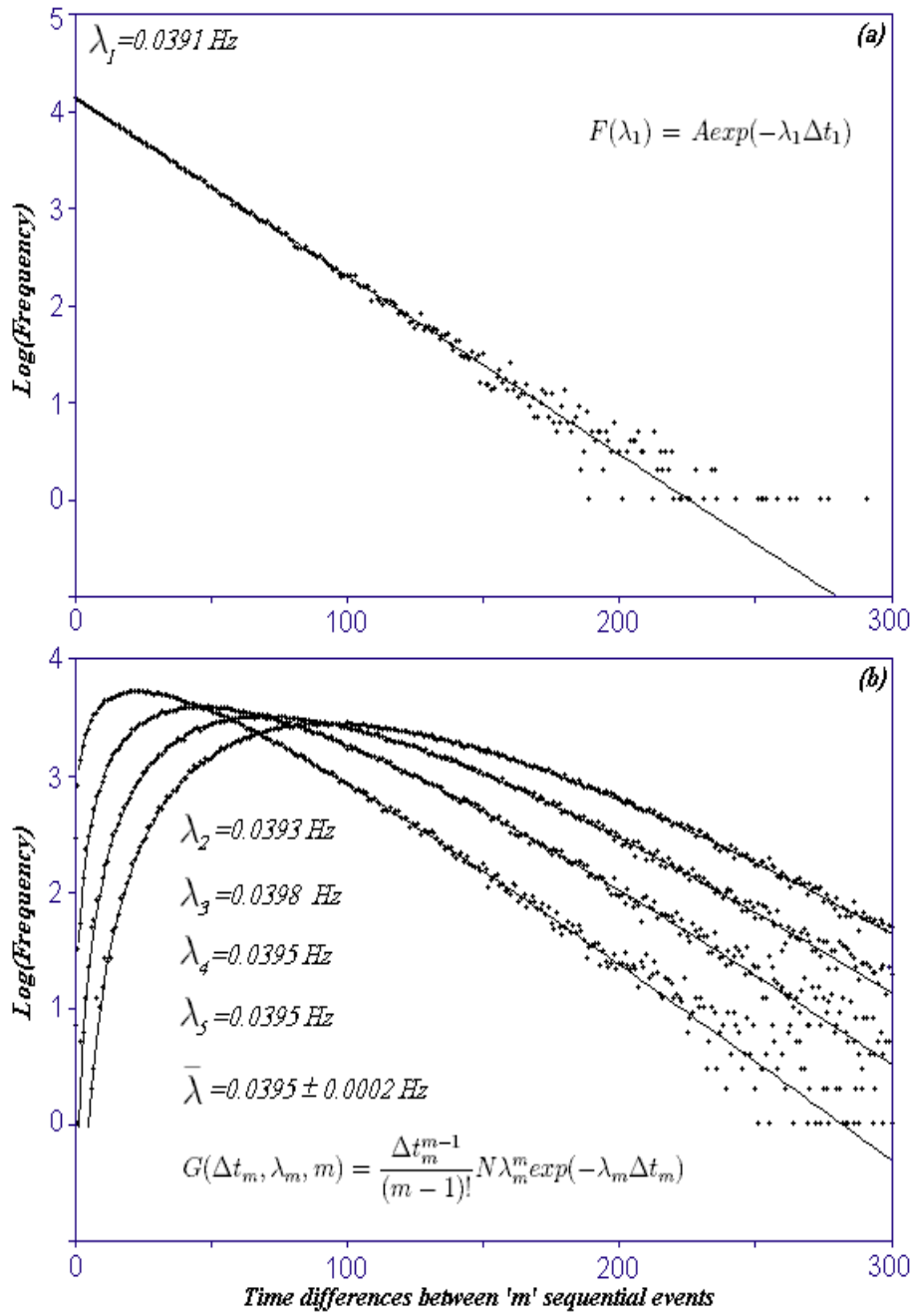


Figure 2: a) The fitted exponential function on the true time(GMT) differences of each two following events. b) Time differences between 2, 3, 4 and 5 sequential events.

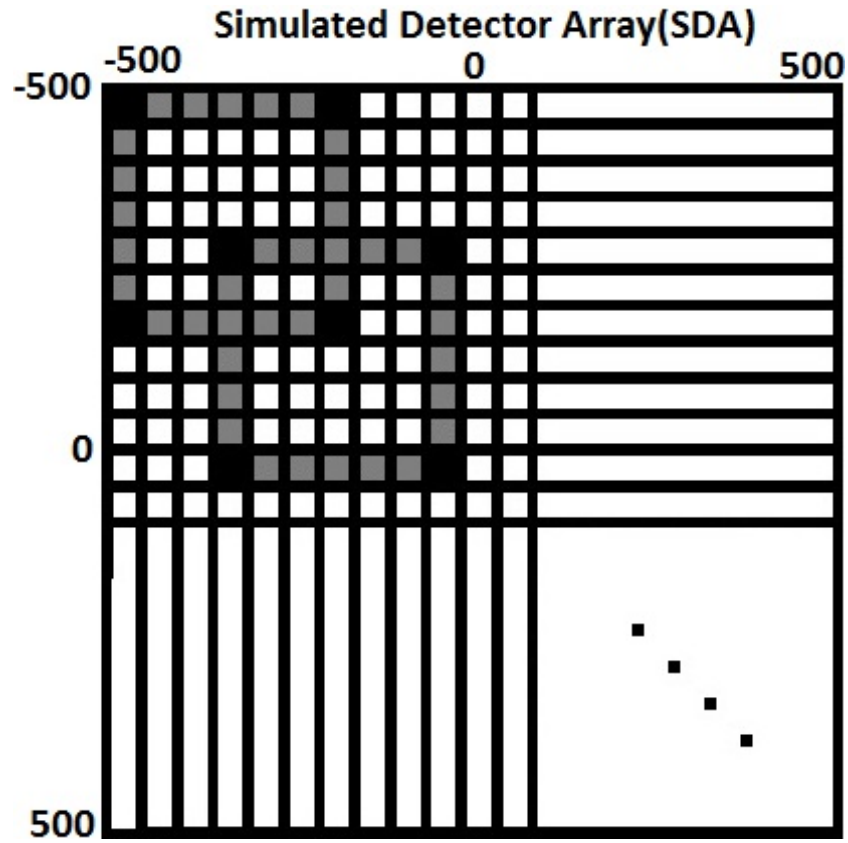


Figure 3: The SDA $(-500:500 \times -500:500)$ with VWCD size $l_{WCD} = \sqrt{A_{eff}}$ meters. In this part it is shown two triggered case samples of the simulation.

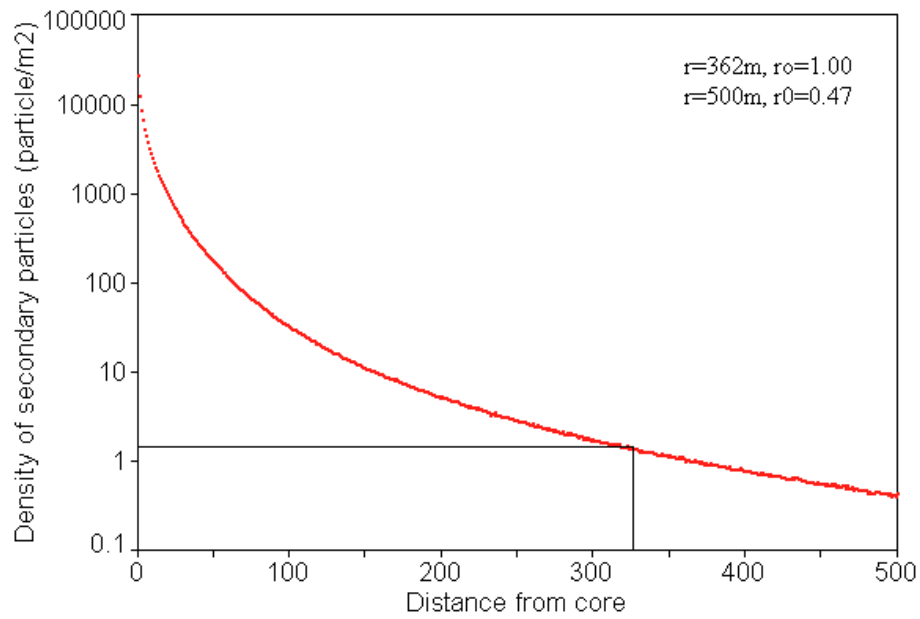


Figure 4: Secondary particle density function in particle/m². WCDs have mean cross section $\bar{A}_{eff} = 0.65\text{m}^2$. Therefore the density $1/0.65 = 1.54$ particles per WCD is the least density which must be considered in our simulation. This radius is $266\text{ m} = 328 \times \sqrt{\bar{A}_{eff}}$. In the simulation it has been considered until $500 \times \sqrt{\bar{A}_{eff}} = 0.47$ particles per each VWCD.

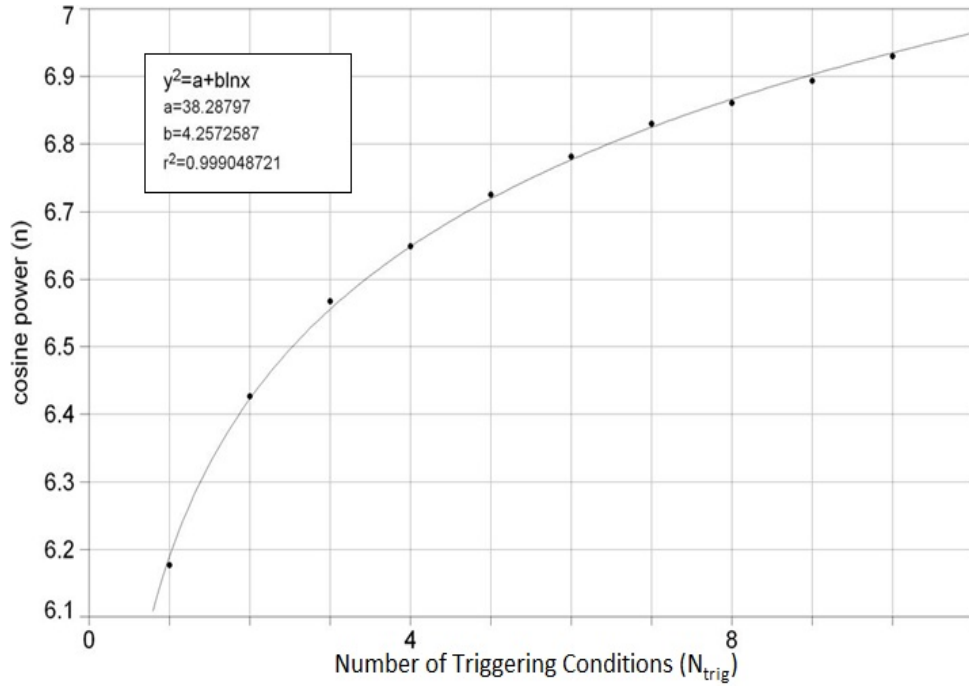


Figure 5: By variation of the lower threshold over N_{trig} and fitting $dN/d\theta$ on the obtained distributions, it is found the first 11 powers (n). Comparison of the simulated results and the experimental results ($n_{exp} = 6.8 \pm 0.1$) shows that, the nearest SE distribution to the experimental data set, is set of SEs with $4.71 \leq N_{trig} \leq 8.93 \equiv N_{trig} \approx 6.82 \pm 2.11$. Therefore detection condition is considered as $N_{trig} \geq 7$.

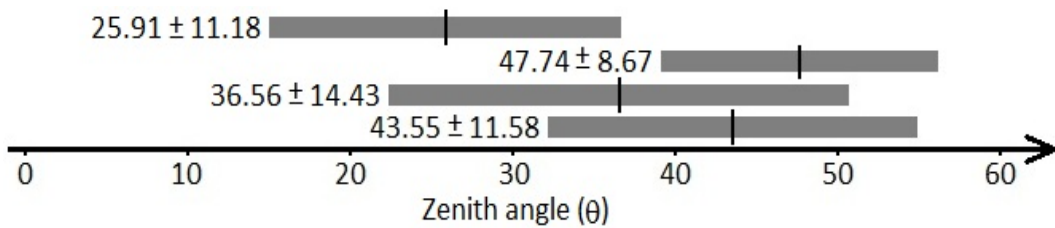


Figure 6: Average zenith angle of: the null SEs is $\bar{\theta}_0 \pm \sigma_{\theta_0} = 43.55^\circ \pm 11.58^\circ$, all SEs have $\bar{\theta}_{tot} \pm \sigma_{\theta_{tot}} = 36.56^\circ \pm 14.43^\circ$, 53,212 high energy null SEs ($E \geq 100$ TeV), $\bar{\theta}_0 \pm \sigma_{\theta_0} = 47.74^\circ \pm 8.67^\circ$, 55,217 high energy ($E \geq 100$ TeV) detectable SEs $N_{trig} \geq 7$, $\bar{\theta}_{det} \pm \sigma_{det} = 25.91^\circ \pm 11.18^\circ$.

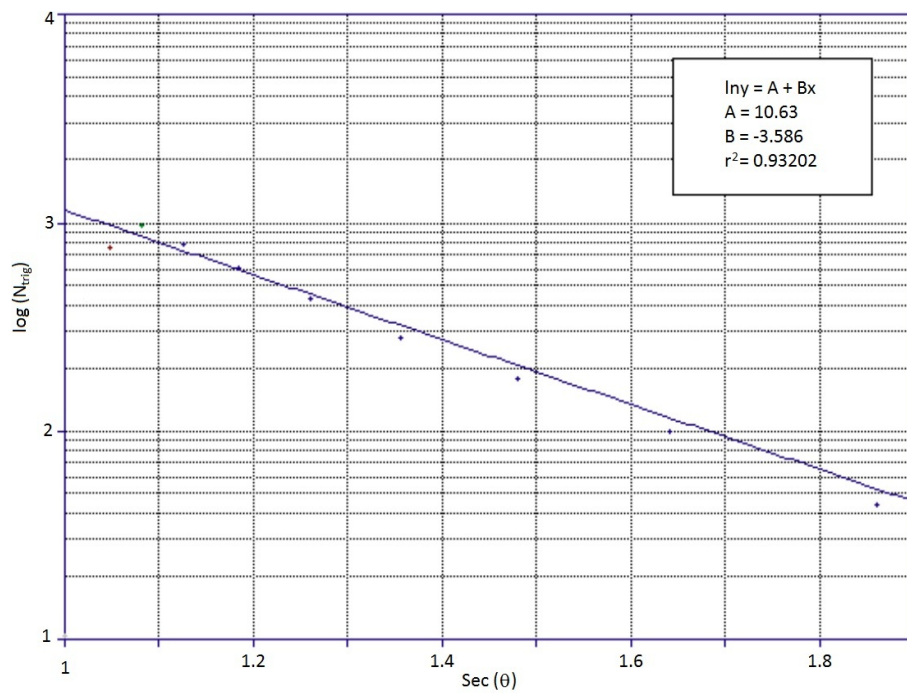


Figure 7: Mean number of N_{trig} vs. $\text{sec}\theta$ of the events with $N_{trig} \geq 7$. The fitted curve is $N_{trig} = N_0 e^{-\tau_0 \text{sec}\theta}$. It is similar to air mass effect on light intensity of stars, which is related to the atmosphere thickness.

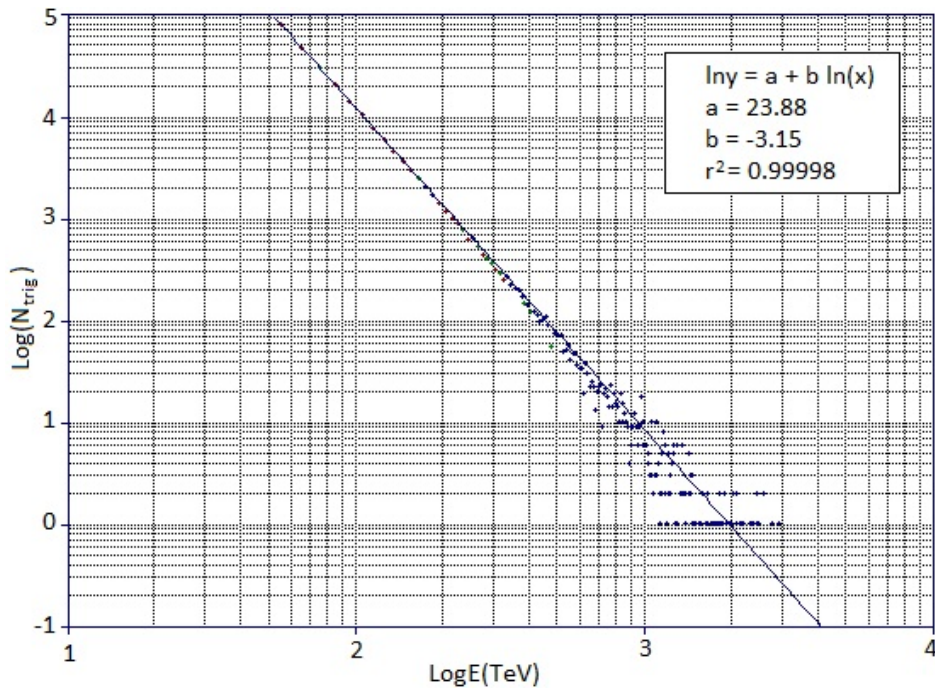


Figure 8: Number distribution of the null events with $N_{trig} = 0$ vs. energy of the simulated events.

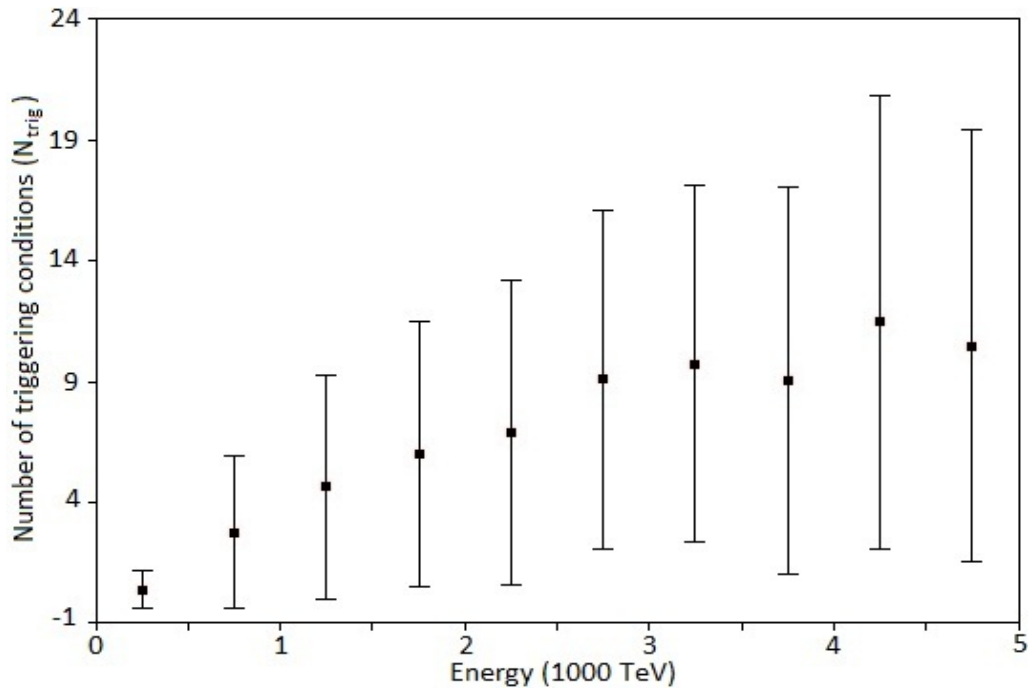


Figure 9: Mean and standard deviation ($\bar{N}_{trig} \pm \sigma_{N_{trig}}$) of the number of triggered cases vs. energy of all of the simulated events.

Acknowledgments

This research was supported by a grant from the national research console of Iran for basic sciences.

Thanks from Dr. M. Bahmanabadi for his helps in this work, and his constructive comments. I acknowledge prof. Paolo Bernardini from University of Lecce and ARGO-YBJ group for our very constructive private communications.

References

- [1] A.A. Watson, *Extensive Air Showers and Ultra High Energy Cosmic Rays* (Summer school in Mexico, 2002).
- [2] L.I. Dorman, *Cosmic rays in the earth's atmosphere and underground* (Cluwer Academic Publisher, 2004).
- [3] T.K. Gaisser, *Cosmic Ray and particle Physics* (Cambridge University Press, 1990).
- [4] K. Greisen *Ann. Rev. Nuc.* 10 (2005), 63.
- [5] P. Sokolsky, *Introduction to Ultra High Energy Cosmic Ray Physics* (Adison-Wesley publishing company Inc, 1989)..
- [6] M. Khakian Ghomi, M. Bahmanabadi, H. Hedayati Kh. *IJAA*, Vol.2, Issue 1 (2015), 97-107.
- [7] A. Borione, M.L. Catanese, M.C. Chantel *et al.* *ApJ* 481 (1997), 313..
- [8] F. Sheidaei, M. Bahmanabadi, M. Khakian Ghomi, F. Habibi, J. Samimi, Y. Pezeshkian and A. Anvari *ICRC.5* (2009)909
- [9] M. Bahmanabadi, A. Anvari, G. Rastegarzadeh, J. Samimi, and M. Lamahi Rächti, *Experimental Astronomy* 8/3 (1998), 211.
- [10] M. Bahmanabadi, M. Khakian Ghomi and F. Sheydaei *astropart. Phys.* 24 (2005), 184.
- [11] A. Marinelli, K. Sparks, R. Alfaro, M. Gonzlez, B. Patricelli, N. Fraija, *NIMPA* 742(2014), 216
- [12] S. BenZvi, *EPJ Web of Conferences*, 105(2015), id.01003
- [13] E. Fuente, T. Ocegüera-Becerra, G. Garca-Torales, J. Garca-Luna, Springer-Verlag Berlin Heidelberg, 34(2013), 439
- [14] F. Sheidaei, M. Bahmanabadi, M. Khakian Ghomi, et al., *ICRC* 5 (2008) 909.
- [15] F. Sheidaei, PhD Thesis., Sharif University of Technology, Tehran, Iran.
- [16] M. Khakian Ghomi, M. Bahmanabadi and J. Samimi, *A&A* 434 (2000), 459.
- [17] F. Sheidaei, M. Bahmanabadi, and J. Samimi, *Astroparticle Physics*, Vol.33, Issue 5-6, 330 (2010).
- [18] David A. Freedman, *Statistical Models: Theory and Practice*, Cambridge University Press (2005)

- [19] M. Bahmanabadi, M. Khakian Ghomi, J. Samimi and D. Pourmohamma, *Experimental Astronomy* 15/1 (2003), 13.
- [20] M. Bahmanabadi, A. Anvari, M. Khakian Ghomi, J. Samimi and M. Lamehi Rachti, *Experimental Astronomy* 13/1 (2004), 39.
- [21] C. Grupen, *Astroparticle Physics* (Springer 2005).
- [22] M. Bahmanabadi, F. Sheidaei, M. Khakian Ghomi and J. Samimi, *Phys. Rev. D* 74 (2006), 08.
- [23] F. Sheidaei, M. Bahmanabadi, A. Keivani, M. Khakian Ghomi, A. Shadkam and J. Samimi, *Phys. Rev. D* 76 082002 (2007).
- [24] D. Heck *et al.*, Report FZKA6019 (Forschungszentrum Karlsruhe) (1998).
- [25] P.K.F. Greider, *Extensive Air Showers* (Springer 2010).
- [26] K. Mitsui *et al.*, *NIM A*290 (1990), 565.
- [27] M. Bahmanabadi, A. Anvari, M. Khakian Ghomi, *et al.*, *Experimental Astronomy*, 13(2002) 39.
- [28] A. Chilingarian, G. Gharagyozyan, G. Hovsepyan and G. Karapetyan; *Astroparticle Physics*, Volume 25(2006), Issue 4, p. 269-276.
- [29] T. Antoni *et. al.*, *Astroparticle Physics*, 19(2003) 703.
- [30] M. Ambrosio *et. al.*, *Astroparticle Physics*, 11(1999) 437-450.
- [31] Jochem D. Haverhoek, Ultra High Energy Cosmic Ray Extensive Air Shower simulations using CORSIKA, April 2006, Leiden University.
- [32] M.T. Dova, L.N. Epele and A.G. Marazzi, *Astropart. Phys.* 18 (2003), 351.
- [33] B.W. Carroll, D.A. Ostlie, *An Introduction to Modern Astrophysics*, (Addison Wesley 2004).